Journal of Microbiological Methods 161 (2019) 87–95

Contents lists available at ScienceDirect

Journal of Microbiological Methods

journal homepage: www.elsevier.com/locate/jmicmeth

Antifungal efficacy of Itraconazole loaded PLGA-nanoparticles stabilized by vitamin-E TPGS: *In vitro* and *ex vivo* studies

Adel A. Alhowyan[a], Mohammad A. Altamimi[b], Mohd Abul Kalam[a], Abdul Arif Khan[a], Mohamed Badran[b], Ziyad Binkhathlan[a], Musaed Alkholief[a], Aws Alshamsan[a,*]

[a] Nanobiotechnology Unit, Department of Pharmaceutics, College of Pharmacy, King Saud University, P.O. Box: 2457, Riyadh 11451, Saudi Arabia
[b] Department of Pharmaceutics, College of Pharmacy, King Saud University, P.O. Box: 2457, Riyadh 11451, Saudi Arabia

ARTICLE INFO

Keywords:
Itraconazole
PLGA
TPGS
Nanoparticles
Nanoprecipitation
Lyophilization
Spray-drying

ABSTRACT

Itraconazole (ITZ) loaded Poly-(D, L-lactic-*co*-glycolic acid, PLGA) nanoparticles (PLGA-NPs) stabilized by D-α-Tocopherol polyethylene-glycol succinate-1000 (TPGS) were developed by nanoprecipitation and single emulsion solvent evaporation methods to improve antifungal activity of ITZ by enhancing its solubility, and hence bioavailability. Encapsulation efficiency, drug loading, *in-vitro* release, *ex-vivo* permeation and antifungal activity were performed for the optimized PLGA-NPs. Characterization of PLGA-NPs were performed by scanning electron microscopy, dynamic light scattering, differential scanning calorimetry, Fourier transform infrared spectroscopy, and powder X-ray diffractometry. We observed that nanoprecipitation method was more efficient in encapsulating ITZ by using 0.3% TPGS (stabilizer) than single emulsion solvent evaporation method. Our thermal analysis studies showed no characteristic peaks for crystalline ITZ, indicating drug efficiently encapsulated inside the nanoparticle with no compatibility issues. Drug loaded PLGA-NPs preserved the antifungal activity of ITZ against *Candida albicans*. Drug release profile from the NPs showed an initial burst release followed by an extended release phase suggesting the potential of NPs for sustained release applications. Furthermore, ITZ encapsulated in PLGA-NPs showed enhanced intestinal permeability in the *ex-vivo* study. In conclusion, the developed nano-system successfully encapsulated ITZ, yielding an increased permeation and consequential antifungal activity.

1. Introduction

Diseases caused by fungal infections have been on the rise from year to year, facilitated by the ease of disease transmission, causing serious illnesses that can be life-threatening (Pinner et al., 1996). Examples of such illnesses include Aspergillosis caused by *Aspergillus*, which can affect lungs, eyes, ears, nails, sinus *etc.* Another example is Tinea, which is primarily caused by *Trichophyton, Microsporum* and *Epidermatophyton* and contributes to most common cutaneous fungal infections (Dutkiewicz and Hage, 2010; Hawksworth, 2001; Richardson, 2005). Treating fungal infections is challenging, especially in patients with underlying diseases due to the lack of efficient drugs. The treatment regimen involves the use of oral or intravenous drugs, which is commonly accompanied with side effects due to the lack of targeting capabilities. Through the processes of absorption, distribution, metabolism, and excretion, much of the active drug circulating through the bloodstream is degraded, renal excreted, or metabolized in the liver. Thus, high doses are needed so the drug exerts its pharmacological action. A notable example in this regard is Itraconazole (ITZ), a broad-spectrum triazole. ITZ is normally prescribed as an oral formulation at doses of 200 mg or 400 mg per day for serious fungal infections, which can lead to potential toxic effects (Bootman, 1998; Islam et al., 2018; Rabinow, 2004; Soppimath et al., 2001). Other azole antifungals, like ketoconazole, voriconazole, fluconazole are also used for various serious fungal infections, however, ITZ exhibits better effectiveness and minimum resistance by many fungal species (Patel et al., 2010). Similarly, amphotericin-B is an alternative common antifungal that is effective in endemic mycoses treatment, but it causes nephrotoxicity as severe side effects (Jung et al., 1999).

ITZ formulation development has been explored previously to produce an efficient system capable of eradicating fungal infections with minimum side effect (Jung et al., 1999; Nakarani et al., 2010; Zong et al., 2017). This task, however, has proven to be complex because of the many challenges associated with ITZ that is mainly due to solubility issues caused by its poor solubility in water ($< 10\,\mu g/mL$) and high log *p* value of 5.66 (Kalam and Alshamsan, 2017). The log p refers to the

* Corresponding author.
E-mail address: aalshamsan@ksu.edu.sa (A. Alshamsan).

https://doi.org/10.1016/j.mimet.2019.01.020
Received 2 December 2018; Received in revised form 29 January 2019; Accepted 31 January 2019
Available online 07 February 2019

logarithm of partition coefficient, which is the ratio of concentrations of unionized species of a compound in a mixture of two immiscible phases at equilibrium. In addition to the poor solubility, ITZ has a plasma protein binding of 99% (Zheng et al., 2012), which greatly affects its pharmacokinetic profile (Heykants et al., 1989). One approach to overcome these issues is by using nanoparticles (NPs) to improve the delivery of the drug. Nanoparticles have shown to be effective drug delivery systems because of their ability to protect the encapsulated drug from degradation by liver, increasing circulation times, bioavailability, absorption, and allowing the control of the drug release (Hans and Lowman, 2002; Leroux et al., 1996). Polymeric NPs have excellent biocompatibility properties, hence they have been used in different applications in areas of gene therapy, protein delivery, and targeted cancer therapies (Fonseca et al., 2002; Nagarwal et al., 2009).

Some of the factors that should be considered in formulating NPs is their particle size, surface charge, and polymer type (Mohamed and van der Walle, 2008). Smaller sized NPs facilitate drug penetration into tissue and are superior in avoiding body's defense mechanisms (Brannon-Peppas and Blanchette, 2004; Desai et al., 1996). In contrast, NPs with a larger particle size are susceptible to opsonization by macrophages, reducing their retention time in circulation. The polymer type, on the other hand, plays an essential role in how the delivery systems react in various environments. Due to the biocompatible nature and controllable release characteristics of synthetic polymers, they have increasingly gained interest in drug delivery. Polylactides (PLA), polyglycolides (PGA), polyanhidrides, and poly (lactide-*co*-glycolide) (PLGA) are some commonly used polymers in drug delivery. PLGA is an FDA approved *co*-polymer that is widely used in drug delivery due to its controllable release characteristics. Achieving this requires altering its degradation rate through varying the molar ratio of lactic and glycolic acid monomers (Mainardes and Evangelista, 2005). During its degradation in physiological fluids, PLGA undergoes hydrolysis of the ester linkages, producing lactic acid and glycolic acid that are normally removed from the body. PLGA is particularly of use for encapsulating drugs that have poor systemic bioavailability due to degradation, clearance, and solubility problems. Entrapment of hydrophobic drugs into polymeric NPs improves drug solubility and allows adequate time for active agents to reach target/infected sites (Zolnik and Burgess, 2007). Synthesis of PLGA NPs can be conducted in the presence of a stabilizer such as vitamin *E*- TPGS (D-α-Tocopherol polyethylene glycol succinate-1000), tween, and polyvinyl alcohol (PVA) creating a stable system that is not prone to aggregation and has enhanced absorptive properties (McCall and Sirianni, 2013).

Here, we describe three methods to prepare PLGA-NPs using vitamin E-TPGS as stabilizer. The use of vitamin E-TPGS offers several possible advantages over other stabilizing agents, including improved emulsification and encapsulation efficiency. TPGS (0.02–0.03%) can have 67-times higher emulsification effects than PVA in the PLGA nanoparticles (Patel et al., 2010; Shieh et al., 2011). Other groups have reported advantages of vitamin E-TPGS, including the inhibition of P-glycoprotein (Binkhathlan and Lavasanifar, 2013), a transmembrane efflux protein, known to contribute to drug resistance by pumping drugs out of target cells. Drug-loaded nanoparticles emulsified with TPGS can achieve higher drug encapsulation efficiency (up to 100%) and cellular uptake, and thus higher therapeutic effects compared with PVA emulsified nanoparticles. The present study attempts to encapsulate ITZ in PLGA-NPs formed with TPGS, improve the functionality of the antifungal activity, and release behavior as compared to free ITZ.

2. Material and methods

2.1. Materials

ITZ was purchased from Beta-Pharma (Shanghai, China). Poly (D, L-lactic-*co*-glycolic acid; PLGA) (50/50, M.W. 45–70 kDa) and D-α-Tocopherol polyethylene glycol succinate-1000 (TPGS) were purchased from Sigma Aldrich (Missouri, United States). Methanol, acetone, dichloromethane and acetonitrile (HPLC grade) were obtained from Fisher Scientific Co. (Loughborough, UK).

2.2. Preparation of NPs (PLGA-NPs)

The PLGA-NPs were prepared using three different techniques: (a) emulsion-solvent evaporation sonicated with an ultrasonicator (US-method) (b) emulsion-solvent evaporation homogenized with an Ultra-Turrax® (UT-method) and (c) nanoprecipitation (Bernabeu et al., 2014).

2.2.1. US-method

ITZ (10 mg) was dissolved in 1 mL of dichloromethane (DCM) containing 100 mg of PLGA to form an organic phase. This organic phase was thereafter added drop-wise to 20 mL of an aqueous solution containing 0.3%, w/v of TPGS. The mixture was sonicated at 40% power to form o/w-microemulsion using a probe sonicator (Badnelin, Germany) for 30 s. The magnetic stirring was continued at room temperature for 3 h for the complete evaporation of DCM and to enhance the ITZ encapsulation within the polymeric matrix of NPs. The developed NPs were further segregated through washing with deionized water by ultracentrifugation at 17,000 rpm for 30 min. The washing step of the precipitant was repeated three times.

2.2.2. UT-method

The same procedure with a slight modification was followed for PLGA-NPs using UT-method. In this case, preparation of NPs was carried out as described above. Then, Ultra-Turrax® homogenization was performed for 20 min to get o/w-microemulsion. The DCM was then removed from the mixture by evaporation under continuous magnetic stirring at room temperature. Afterwards, the developed NPs were treated as described in the US-method.

2.2.3. Nanoprecipitation method

PLGA (100 mg) and ITZ (10 mg) were dissolved in 10 mL of acetone. This polymer mixture was added drop-wise to 20 mL of 0.3%, w/v TPGS solution (in 10 mM citrate buffer; pH 5). The suspension was then kept under continuous magnetic stirring for 3–4 h for the complete evaporation of the organic phase (acetone). Then, the NPs were treated as described in the US-method. Then, the NPs precipitant was dispersed in aqueous solution by vortexing for 30 s and either frozen at −70 °C for lyophilization or spray dried. Finally, the resulted NPs were kept at 4 °C for further use.

2.3. Particle size, polydispersity and zeta-potential measurement

The particle size, polydispersity index (PDI) and zeta-potential of the NPs were measured by a Zetasizer Nanoseries-ZS (Malvern Instruments, UK). Dynamic light scattering (DLS) mode was used to measure the particle size and size distribution (PDI) of NPs at 25 °C after proper aqueous dilution. Laser Doppler Velocimetry (LDV) mode of the same instrument was used for determination of zeta potential (mV) of the NPs after an appropriate dilution with distilled water at 25 °C. All experiments were performed in triplicate.

2.4. Particle morphology by SEM

The shape and surface characteristics was observed by micrographs of the samples taken by scanning electron microscopy (SEM) (Zeiss EVO LS10; Cambridge, United Kingdom and FESEM (JSM-7600F, JEOL Inc., Akishima, Japan)) using gold sputter technique. The NPs were vacuum dried coated with gold in a Q150R Sputter unit from Quorum Technologies Ltd. (East Sussex, UK) for 60 s in an argon atmosphere at 20 mA. The zone magnification for the images were kept around 10,000–15,000×. Observations were performed under 1 and 15 kV

(Akhtar et al., 2017; Kalam et al., 2017).

2.5. Differential scanning calorimetry (DSC)

Physical state analysis was conducted using a DSC-8000 (Perkin Elmer Instruments, Shelton, CT, USA) at a scan rate of 10 °C/min. Samples of 2–3 mg were weighed and placed in aluminum pans and lid was crimped to form a hermetic seal (Altamimi and Neau, 2016). The DSC was calibrated with indium (100% pure, melting point 156.60 °C, heat of fusion 6.80 cal/g). The sample and reference cells were purged with nitrogen at 20 mL/min. The results were analyzed using PYRIS *V*-11 software. The thermal behavior of the samples was investigated at a scanning rate of 10 °C/min with the temperature range of 25–200 °C.

2.6. Fourier transform infrared spectroscopy (FTIR)

The FTIR spectrum of the drugs, the polymers, and their lyophilized or spray dried NPs were obtained using a Perkin Elmer (FTIR) spectrum BX. The materials were prepared as potassium bromide (KBr) pellets and spectra were collected across 4400 to 350 cm^{-1} wavenumber using 3 scans and 2 cm^{-1} resolution (Sathigari et al., 2012).

2.7. Powder X-ray diffraction (PXRD)

Diffraction patterns were analyzed on an Ultima-IV diffractometer (Rigaku, Tokyo, Japan) over a 2θ range from 3 to 60° at the rate of 0.5°/min scan speed. The tube anode was Cu with Ka = 0.1540562 nm monochromatized with a graphite crystal. The pattern was collected at 40 kV of tube voltage and 40 mA of tube current in step scan mode (step size 0.02°, counting time 1 s per step) (Modi and Tayade, 2006).

2.8. Encapsulation efficiency (%EE) and drug loading capacity (%DL)

EE% and DL%of NPs were calculated by centrifuged suspension of NPs at 12,000 rpm for 30 min at room temperature. Then, supernatant was discarded and the obtained pellets were dissolved in dichloromethane (DCM). Then the DCM was evaporated under vacuum. Later, pellets were dissolved in methanol and analyzed by HPLC at 261 nm. The EE% and DL% were calculated by using the following equations.

$$EE\% = \frac{(Amount\ of\ ITZ\ loaded\ in\ NPs\ (mg))}{(Total\ amount\ of\ ITZ\ used\ (mg)} \times 100 \quad (1)$$

$$DL\% = \frac{(Amount\ of\ ITZ\ loaded\ in\ NPs\ (mg))}{(Total\ Amount\ of\ formulation\ (mg))} \times 100 \quad (2)$$

2.9. HPLC analysis of ITZ

ITZ amount in the prepared NPs was determined by using a slightly modified reverse phase-HPLC-UV method (Alomrani et al., 2014). The HPLC system (Waters™ 600 controller, USA) equipped with pump (Waters™ 1252 a Binary pump, USA), wavelength detector (Waters™ 2487 a dual λ Absorbance detector, USA), and an automating sampling system (Waters™ 717 Plus Auto- sampler, USA) was used. The HPLC system was monitored by "Empower (Water)" software. ITZ was analyzed using mobile phase consisting of deionized water:acetonitrile (30,70 v/v). The mobile phase flowed over a reversed-phase C_{18} column (μBondapak™, 4.6 × 150 mm, 10 μm particle size, Waters) at the rate of 1.2 mL/min. The injection volume of each ITZ sample was 30 μL and detected by UV-detector at 261 nm. All the operations were carried out at room temperature.

2.10. In vitro drug release

In vitro release studies were conducted on the three formulations: nanosuspension prepared by nanoprecipitation (optimized formulation before drying), lyophilized and spray dried PLGA-TPGS NPs. All formulations containing a 10%, *w*/w theoretical loading of ITZ. The release study was carried on 0.1 N HCl solution in the first 2 h then in PBS (pH 6.8) containing sodium lauryl sulphate (0.5%, w/v solution) to insure the sink condition for 72 h. The NPs was dispersed in the dialysis membrane (MWCO = 12 kDa) then immersed in beakers contaning 400 mL of release media then beakers were placed in a shaking water bath at 37 ± 1 °C and 50 rpm. At scheduled time points, 1 mL of sample from the release medium was collected and filtered through 0.45 μ membrane filter. Then, same volume of fresh release medium was added to the beaker containing release medium to maintain the sink condition. The amount of drug released was quantified by HPLC-UV method as described above. All experiments were performed in triplicate.

2.11. Ex vivo intestinal permeation

Small intestine was immediately excised and placed into Krebs buffer solution directly after sacrificing male Wistar rats weighing 200–250 g. All studies were in accordance with the Guidelines of Animal Ethical Committee of King Saud University. The tissue was cut into accurately measured segments and rinsed with ice-cold Krebs buffer to remove luminal content. Suspension of NPs (1 mL) was placed in lumen of intestine that was tied from one side and then tied from the other side. The composition of the Krebs solution (pH 6.5) was 0.34 g/L potassium chloride, 1.8 g/L glucose, 7 g/L sodium chloride, 0.207 g/L sodium dihydrogen phosphate, 0.251 g/L disodium hydrogen phosphate and 46.8 mg/L magnesium chloride. Constant temperature with continuous aeration of 37 ± 0.5 °C were maintained. At predetermined time interval samples were taken from the receptor chamber and replaced with an equal volume of fresh buffer. Aliquots were assayed for the drug content using HPLC at 261 nm. Apparent permeability coefficient (P_{app}) and permeability enhancement ratio were calculated from the Eqs. (3) and (4), respectively.

$$Papp = \frac{dQ}{(dt \times A \times Co)} \quad (3)$$

Where A is the area of the tissue (cm^2), dQ/dt is the steady-state appearance rate on the acceptor side of the tissue and C_o is the initial concentration of the drug in the donor compartment (Binkhathlan and Lavasanifar, 2013).

$$Permeability\ Enhancement\ ratio = \frac{Papp\ of\ the\ NPs\ formulation}{Papp\ of\ the\ drug\ solution} \quad (4)$$

Ex vivo studies were conducted and compared for three preparations: nanosuspension prepared by nanoprecipitation (optimized formulation before drying), ITZ-aqueous suspension, and ITZ in 0.3% TPGS. All formulations contained the same amount of ITZ.

2.12. Antifungal activity

The antifungal activity of ITZ loaded PLGA-NPs was tested on fungal growth inhibition zone. Growth inhibition zones were calculated on a lawn of *Candida albicans* ATCC 90028 in a petri plate using disc diffusion assay with 5 mm discs. ITZ-loaded PLGA-NPs were compared against ITZ-aqueous suspension for antifungal activity (Alomrani et al., 2014). Empty PLGA-NPs were used as a control. All experiments were performed in triplicate using Mueller Hinton Agar media.

2.13. Physical stability study

For physical stability study, ITZ-loaded PLGA-NPs prepared by US-method and nanoprecipitation method were stored at room temperature (30 ± 1 °C) for 3 months in stoppered glass vials by following reported methods (Kalam et al., 2017; Li et al., 2017). Samples were

periodically evaluated for particle size, zeta-potential, polydispersity, encapsulation and drug loading to evaluate the physical stability of the NPs (Kalam et al., 2017; Li et al., 2017). The quantification of the drug was done by previously used HPLC-UV method.

3. Statistics

The results were articulated as mean ± SD and analyzed for statistical significance ($p < .05$) by Paired *t*-test (GraphPad Software Inc. San Digeo, USA).

4. Results and discussion

4.1. Formulation and characterization of ITZ-loaded NPs

The aim of our study was to obtain ITZ-PLGA NPs stabilized with TPGS using three different methods depending on the solubility characteristics of the selected polymer. Both ITZ and PLGA were readily soluble in acetone, and DCM, producing NPs. In case of nanoprecipitation, acetone was used because of its solubilization capacity of the used components and its miscibility with water. In addition, acetone can be removed easily by evaporation under mechanical stirring over a short time. In case of US- and UT-methods, DCM was used due to its ability to form stable single emulsion through sonication or homogenization (Sahana et al., 2008). The selection of the optimal formulation is based on higher encapsulation, uniform size distribution, spherical morphology, higher zeta-potential *v*alue, and higher drug loading. In our attempt to select for the optimal formulation we used different concentrations of TPGS (0.03, 0.01, 0.1 and 0.3%, w/v) and different amounts of PLGA (50, 100 and 150 mg). Ultimately, a concentration of 0.3%, w/v of TPGS and 100 mg of PLGA resulted in the best optimized formulation in all the three applied formulation development methods. Notably, lower concentrations of TPGS have been used successfully in the literature (Bernabeu et al., 2014).

NPs size and Zeta potential have a determining effect on the formulation stability, drug release, and cellular uptake (Desai et al., 1996). Data showed that nanoprecipitation and US-method produced smaller particles with uniform distribution (unimodal) compared to the UT-method (Table 1). However, no significant difference was found between the size of the particles obtained from nanoprecipitation and US-methods. NPs resulting from the UT-method were not used in the subsequent analysis due to their large particles sizes, bimodal distribution, and inability to detect the drug within NPs. Negative zeta potential values of ITZ-PLGA NPs are attributed to the presence of the ionized hydroxyl groups of PLGA and TPGS. The highest zeta potential value of the PLGA-NPs was found to be around −24.7 mV when prepared by nanoprecipitation method, while it was −16.8 mV when prepared by US-method. Such significant difference in zeta potentials between nanoprecipitation and US-method indicated that the nanoprecipitation method produced more stable NPs. A visualization of the NPs can be observed in the SEM microphotographs (Fig. 1), where drug crystals were not detected around the NPs or on the surfaces, suggesting that the drug was completely encapsulated. In addition, all NPs formulations were spherical in shape with smooth surfaces.

4.2. DSC analysis

According to the literature, ITZ has a melting point of 162.53 °C, PLGA has a glass transition temperature (T_g) of 45.30 °C, and TPGS has a melting point of 35.28 °C (Gajra et al., 2015; Gaonkar et al., 2017). Lyophilization and spray drying techniques were used to obtain solid form of PLGA-NPs. Lyophilized NPs (Fig. 2D), which were prepared using nanoprecipitation method, showed broader melting endotherms for PLGA and TPGS with no melting peak for ITZ, indicating that drug was in amorphous form and most of the drugs were encapsulated into the core of the NPs. Spray dried NPs, on the other hand, showed no crystalline melting endotherms for ITZ, while both melting temperature and glass transition temperature were lowered indicating more efficient dispersion between the components resulting in complete miscibility. Additionally, no additional peaks were observed indicating that the excipients were compatible with the drug (Altamimi and Neau, 2017; Mainardes and Evangelista, 2005). SEM images, however, showed agglomerated particles resulting in a dramatic increase in the size and difficulties when trying to re-suspend the particles. It is important to note that the use of cryoprotectent is essential to obtain successful lyophilization or spray drying to produce particles in nanosize range.

4.3. FTIR analysis

Most chemical substances have their molecular bonds stretched or bent under FTIR energy yielding a specific IR spectrum, which serves as a fingerprint that is widely utilized to identify functional groups and newly formed chemical bonds (Huang et al., 2008). FTIR analysis for pure ITZ (Fig. 3a) showed distinctive peaks at 1378.15, 1750, 1100 cm^{-1}. As for the peaks around 3000 cm^{-1}, they were formed due to stretching vibration of -NH_2 group. The –OH functional group showed different peaks at 3600 cm^{-1} (Nesseem, 2001; Tao et al., 2009). PLGA (Fig. 3b) showed –OH stretching with characteristic peak around 3500 cm^{-1} (Mainardes and Evangelista, 2005), while TPGS (Fig. 3c) has a carbonyl band (-C=O) at 1750 cm^{-1}. The spectra of PLGA-NPs have shown the characteristic peaks of ITZ at 1378.15, 1750, 1100, 3000, 3600 cm^{-1}. Also, they showed the characteristic peaks of PLGA and TPGS and no formation of new peaks. Therefore, drug and excipients are compatible with each other and revealed that ITZ was successfully incorporated into the PLGA-NPs.

4.4. PXRD analysis

The spectra of X-ray diffractometry for pure compounds and the formulated NPs are presented in Fig. 4. The X-ray diffractogram of ITZ shows a typical crystalline pattern with prominent sharp peaks at diffraction angles of (2θ) 14.50°, 17.50°, 18.00°, 20.40°, and 23.50° (Jung et al., 1999), and intensity values above 1000 cps. For PLGA (Fig. 4b) no sharp peaks were found, only a halo pattern was obvious indicating a completely amorphous form, which was confirmed earlier by DSC analysis. PGS has two characteristic two sharp peaks at diffraction angles 19.40° and 23.60° (Wang et al., 2016). In the lyophilized NPs, we found some peaks with much reduced intensity related to ITZ and TPGS. Fig. 4e shows only TPGS characteristic peaks indicating that

Table 1
Particle size, polydispersity index, and zeta potential of ITZ-loaded PLGA- NPs stabilized by TPGS and the results were presented as mean ± SD, $n = 3$.

Parameters	Nanoparticles preparation methods		
	Single emulsion evaporation/homogenization (UT-method)	Single emulsion evaporation/sonication (US-method)	Nanoprecipitation method
Percentage yield (%)	50.00	50.00	70.00
Particle size (nm)	349.45 ± 23.55	213.15 ± 12.51	176.96 ± 24.32
Polydispersity index	0.531 ± 0.004	0.431 ± 0.101	0.212 ± 0.041
Zeta potential (mV)*	−6.88 ± 1.23	−16.8 ± 1.69	−24.7 ± 1.04

* Indicate a significant difference of ($p < .05$) between the methods.

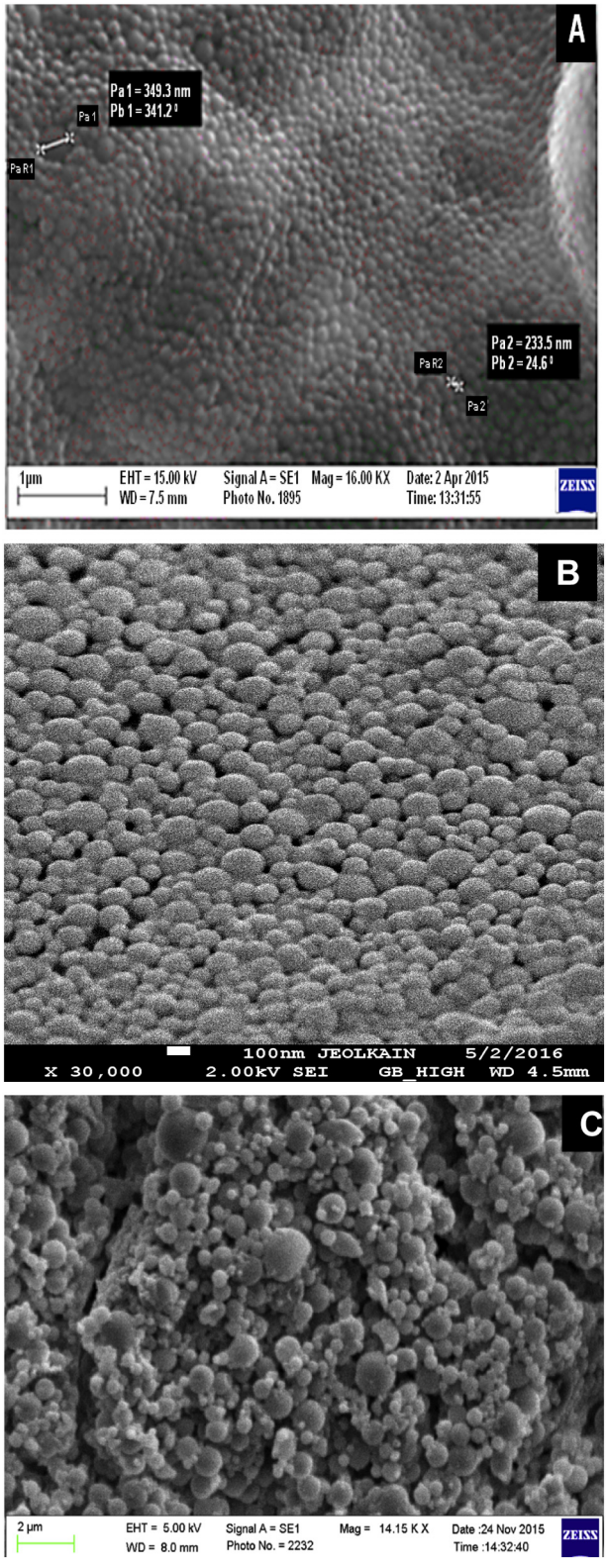

Fig. 1. Scanning electron microscopy images showing the morphology of (a) empty lyophilized NPs prepared by nanoprecipitation, (b) ITZ-loaded lyophilized NPs prepared by nanoprecipitation (c) ITZ-loaded lyophilized NPs prepared by US-method.

spray drying technique was superior to lyophilization when rendering the drug completely amorphous. Such superiority is attributed to the rapid drying process compared to the lyophilization technique.

4.5. Encapsulation efficiency and drug loading capacity

Using nanoprecipitation method, the encapsulation efficiency of ITZ was 94.25% while the US-method yielded a value of 50.38% (Table 2). In addition, DL% for the nanoprecipitation method was 6.37% compared to 2.15% for the US-method (Table 2). Such a significant difference ($p < .05$) might be attributed to the more efficient stabilization of NPs by nanoprecipitation method. The use of slightly acidic medium of pH = 5 facilitated the ionization of ITZ and the consequent increase in its solubility and dispersion in comparison to intrinsic aqueous solubility of ITZ (0.00964 mg/mL), resulting in increased drug content and drug encapsulation *v*alues (Heykants et al., 1989). Although other groups have reported higher encapsulation efficiency and drug loading for some insoluble drugs using TPGS (0.03%, *w/v*) by the US-method (Bernabeu et al., 2014), we report that the nanoprecipitation method was superior in producing PLGA-NPs with higher EE% and DL% of ITZ. This could be due to ITZ escaping the emulsification step with the organic solvent to the aqueous phase leading to ineffective entrapment in the polymeric matrix. Avoiding emulsification seems efficient in increasing ITZ disposition in the instantly-precipitating NPs increasing the encapsulation of ITZ in PLGA-NPs (Alshamsan, 2014). It is noteworthy to mention that the UT-method resulted in no encapsulation of drug in the NPs. Taken together, PLGA-TPGS based NPs prepared by nanoprecipitation method were selected for further studies such as *in vitro* drug release, antifungal activity and intestinal permeability.

4.6. In vitro drug release

In vitro release profile from optimized formulation, lyophilized and spray dried PLGA-TPGS NPs was studied (Fig. 5a). A certain volume of the prepared nanosuspension or exact weighed amount of dry NPs either lyophilized or spray dried in a dialysis bag. It was found that the suspension of PLGA-NPs (before drying) exhibited biphasic release in the simulated biological fluid, with an initial burst release of about 31.88% after 6 h. The other phase was a steady state release profile with about 45.01% of drug released after 72 h. Such an initial fast release, usually known as burst effect, is due to the release of unencapsulated or loosely bound drugs present on the surface of NPs (Patel et al., 2010). After initial burst release, release of ITZ from PLGA-NPs occurred through the combined effects of diffusion and particle degradation phenomenon (Patel et al., 2010). It is worth pointing out that the second phase of the release could be utilized to increase the biological half-life and decrease the frequency of dosing. The release of ITZ in second phase of release process took place by diffusion and hydrolytic degradation of PLGA matrix to glycolic and lactic acid (McCarron et al., 2006; Mittal et al., 2007). From this profile, it was apparent that a steady dose of ITZ could be administered over three consecutive days, resulting in increasing the efficacy of ITZ over this time period. On the other hand, it was clear that the release of ITZ from lyophilized and spray dried PLGA-NPs was inadequate with 3.01% and 15.31% cumulative amount at 72 h, respectively. Such slight but significant increase in the drug release of spray dried particles could be attributed to the complete miscibility of ITZ in polymeric matrix, which was proven earlier with the powdered X-Ray diffractometry analysis (Papadimitriou and Bikiaris, 2009).

4.7. Ex vivo drug permeation experiment

Ex vivo permeability study indicated higher apparent permeability (P_{app}) for ITZ loaded NPs as compared to free ITZ (Fig. 5b). Permeation of NPs was observed at each time point and the P_{app} for the ITZ-loaded PLGA-NPs was found to be 3.2×10^{-4} cm·s^{-1}, which was significantly higher ($p < .05$, approximately 5-folds) as compared to free ITZ (0.63×10^{-4} cm·s^{-1}). Apparent permeability for the ITZ-TPGS suspension was found to be 1.09×10^{-4} cm·s^{-1}, ($p < .05$, approximately 2-folds) (Gajra et al., 2015). Furthermore, around 58.37% of ITZ

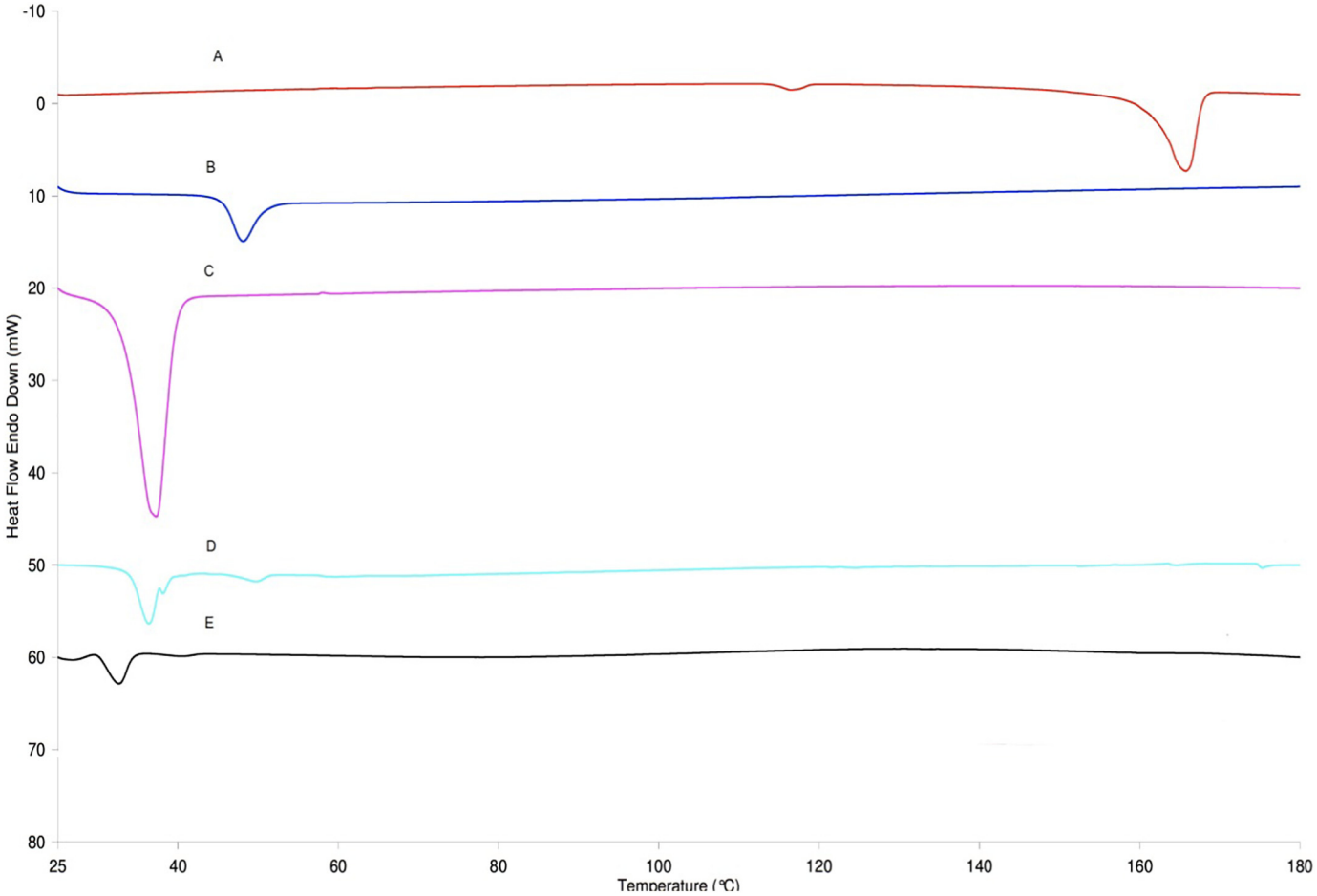

Fig. 2. Overlaid DSC thermograms for (A) Itraconazole, (B) PLGA, (C) TPGS, (D) lyophilized NPs, and (E) spray dried NPs. The thermograms of the NPs did not show the melting peak for the Itraconazole at around 162.53 °C, illustrating that the drug was in the amorphous state rather than in crystalline state and drug was completely encapsulated within the core of the NPs.

permeated across the intestinal membrane at 4th h, which was significantly high as compared to ITZ-aqueous suspension, which was only 9.53% at the same time point. The intestinal permeation of ITZ was approximately 2-fold higher when the drug was suspended in 0.3% TPGS solution only, which could be due to the inhibition of p-glycoprotein in the intestine by TPGS (Binkhathlan and Lavasanifar, 2013).

4.8. Antifungal activity

Antifungal activity was performed using either empty PLGA-NPs, ITZ aqueous suspension, or ITZ-loaded PLGA-NPs against *Candida albicans* (strain ATCC 90028) through the disc diffusion assay method. The empty NPs had no obvious inhibitory action against the fungal growth. A significant increase in the zone of inhibition from ITZ-loaded PLGA-NPs and ITZ aqueous suspension was found as compared to empty NPs. The difference in the inhibition between ITZ aqueous suspension and ITZ-loaded PLGA-NPs was significant ($p < .05$) with larger inhibition zone of NPs (Fig. 6). The larger zone of inhibition of drug loaded NPs might be attributed to the capability of PLGA-NPs to infiltrate across the surrounding media and fungal spores (Qiu et al., 2015). Moreover, the sustained release of ITZ explains the larger inhibition zones observed over time with the ITZ-loaded PLGA-NPs as compared to ITZ aqueous suspension. The reason behind this might be the smaller size of the NPs and its uniform aqueous dispersibility that have increased the contact duration of the NPs with the spores and cells and lead to rapid drug internalization (Patel et al., 2010). This experiment proved that ITZ when encapsulated in PLGA-NPs preserved its antifungal activity without any alteration in the intrinsic property of the ITZ molecule due to the processing effects.

A study involving preparation of monomethoxypoly (ethylene glycol)-*b*-poly(lactic acid) (mPEG-*b*-PLA) based ITZ loaded nanoparticles and the results of the study found that the nanoparticles effectively inhibited fungi *in vitro* and *in vivo*, but their formulation was for IV administration which caused mild venous irritation and slight hemolysis (Ling et al., 2016). The present ITZ loaded NPs are intended for oral use so there will be no chance of such adverse events. Another study showed preparation of ITZ loaded PLGA NP and performed their antifungal activity against *Aspergillus flavus* and found clear inhibition zone at 0.3 mg/mL ITZ and small inhibition zone at 0.03 mg/mL of ITZ, but we found antifungal activity after adding at 100 μg/mL ITZ against *C. albicans* (Patel, 2010). In addition, Alomrani et al., 2014 prepared ITZ loaded liposomes and found that the antifungal activity of drug loaded liposome was same as compared to drug solution (Alomrani et al., 2014). Our study found that the activity of ITZ-loaded PLGA-NPs was more than ITZ suspension suggesting that NPs may be promising for the development of an effective formulation.

Above findings represent some promising advantages of using TPGS stabilized PLGA NPs loaded with ITZ against previously developed nanoformulations.

4.9. Stability studies

To check prolonged shelf-life and physical or storage stability, the prepared ITZ-loaded PLGA-NPs we performed stability study at room

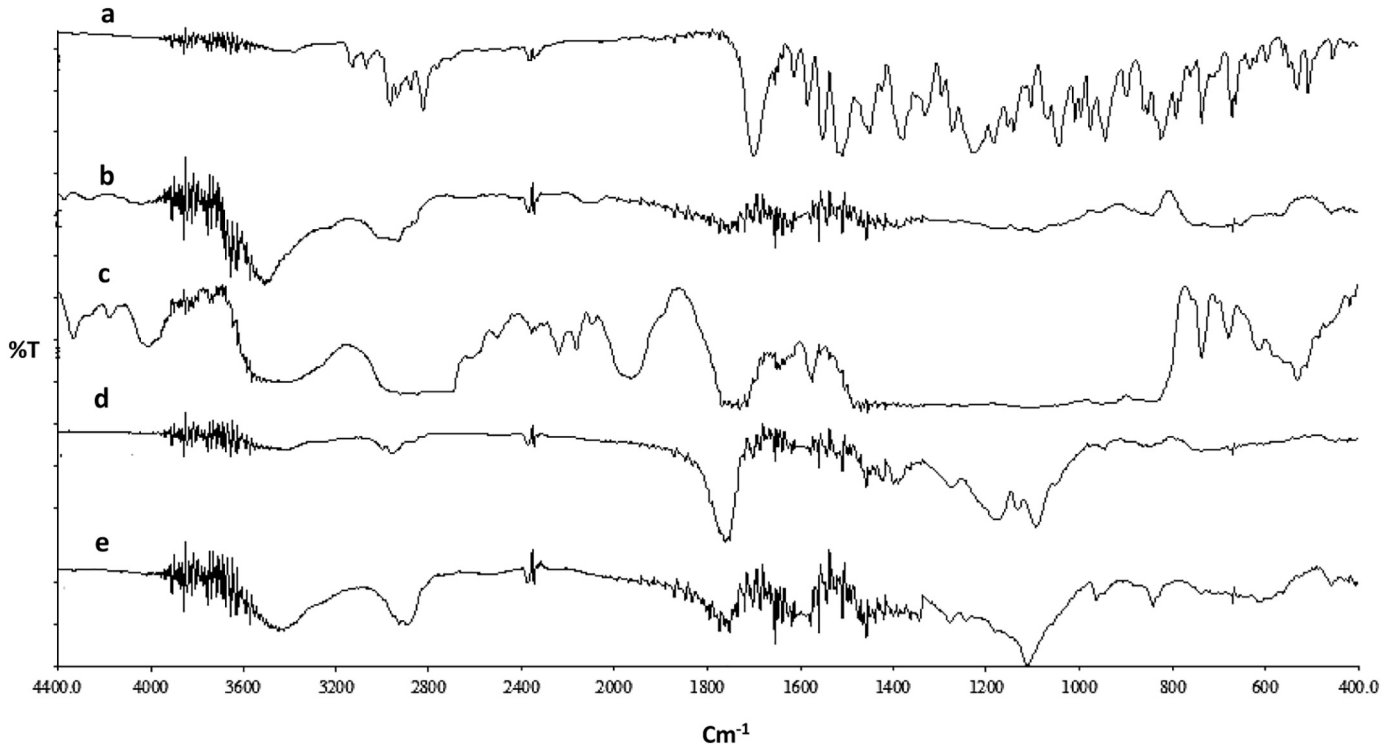

Fig. 3. The stacked Infrared spectra of (a) Itraconazole (ITZ), (b) PLGA, (c) TPGS, (d) lyophilized NPs, and (e) spray dried NPs. There was no formation of any new peak at the wave numbers of functional groups of ITZ, indicating that ITZ and the excipients are compatible with each other and revealed that ITZ was successfully encapsulated within the matrix of PLGA.

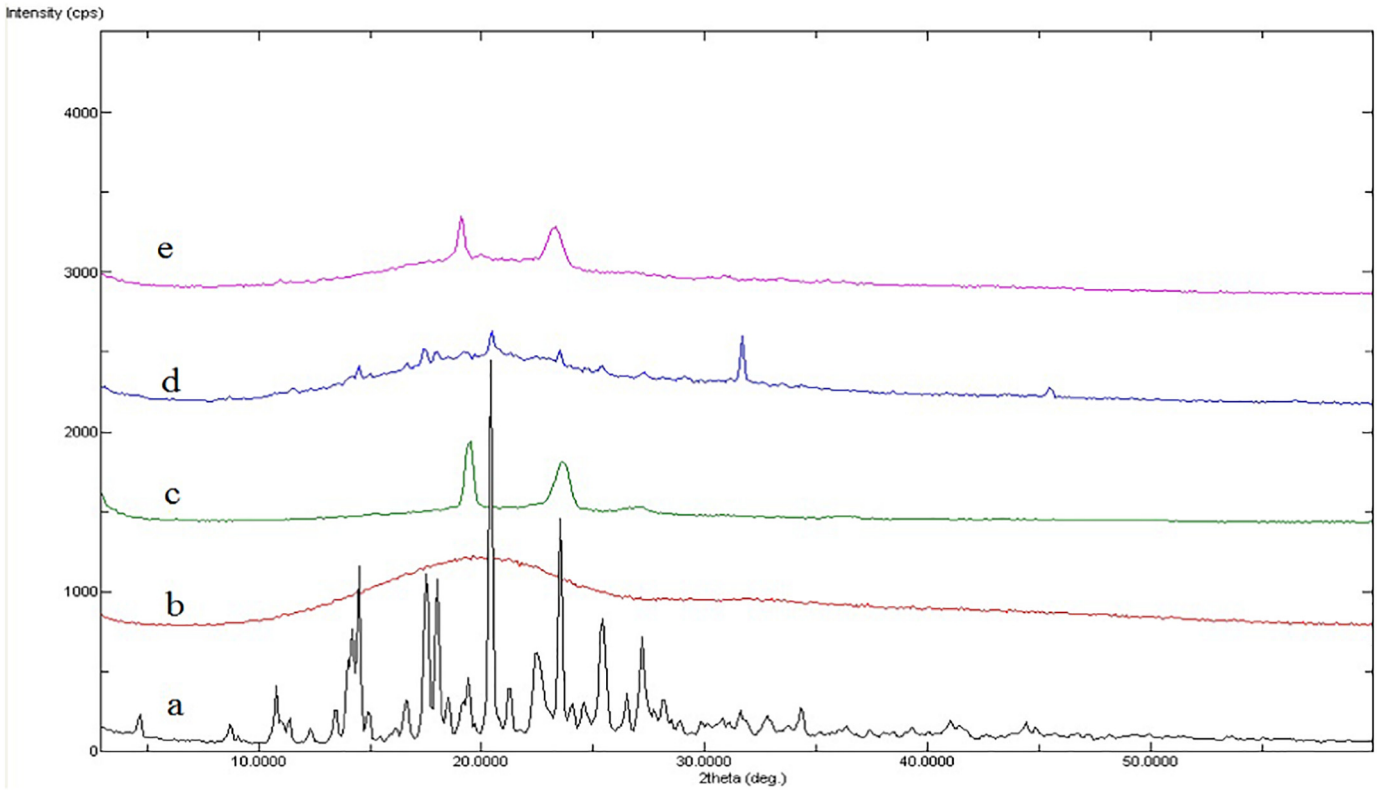

Fig. 4. Overlaid PXRD patterns: (a) Itraconazole (ITZ); (b) PLGA, (c) TPGS (d) lyophilized NPs, and (e) spray dried NPs. The reflections of pure ITZ were sharp, while the lyophilized and spray dried NPs presented low intensity reflections with higher Bragg's spacing at different 2θ angle, illustrating that the ITZ in lyophilized NPs was less crystalline as compared to the pure ITZ. The drug peak was not found in spray dried NPs. Low intensity reflections and absence of ITZ peaks in the diffractogram of NPs indicated that the ITZ was encapsulated within the matrix of polymer.

Table 2
Effect of storage on particle size, polydispersity, zeta potential, encapsulation and drug loading on ITZ-loaded PLGA-NPs for 3 month at 30 ± 1 °C temperature and the results were presented as mean ± SD, $n = 3$.

Duration of storage	Particle size (nm)	Polydispersity index (PDI)	Zeta potential (mV)	Encapsulation efficiency (%EE)	Drug loading (%)
At the time when PLGA-NPs were prepared					
US-method	213.15 ± 12.51	0.431 ± 0.101	−16.81 ± 1.06	50.38 ± 3.65	2.15 ± 1.08
Nanoprecipitation method	176.96 ± 24.32	0.212 ± 0.041	−24.72 ± 1.54	94.25 ± 5.45	6.37 ± 1.75
After 1 month					
US-method	234.12 ± 9.85	0.438 ± 0.087	−13.15 ± 0.99	48.25 ± 2.36	2.13 ± 1.03
Nanoprecipitation method	183.45 ± 8.19	0.219 ± 0.016	−20.32 ± 1.08	90.62 ± 3.75	6.28 ± 1.23
After 3 months					
US-method	257.86 ± 12.15	0.445 ± 0.071	−12.09 ± 1.28	45.48 ± 1.97	2.07 ± 1.12
Nanoprecipitation method	192.53 ± 10.75	0.223 ± 0.008	−18.45 ± 1.97	85.24 ± 2.09	6.23 ± 1.19

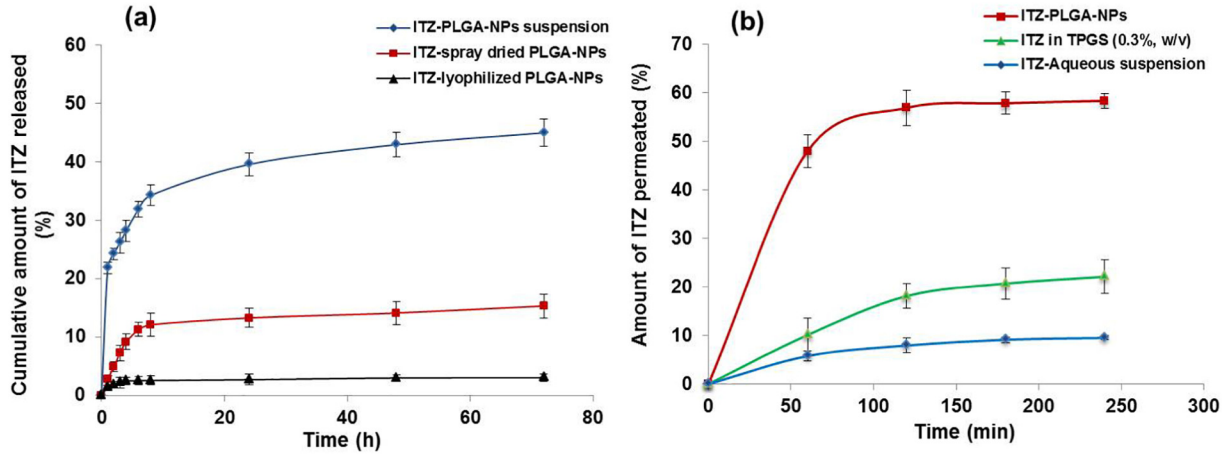

Fig. 5. *In vitro* drug release profiles of drug loaded-NPs lyophilized and spray dried NPs (a); Total permeable amount (%) comparison between ITZ-aqueous suspension, ITZ loaded NPs and ITZ in 0.3% TPGS (b). Results were represented as mean ± SD, $n = 3$.

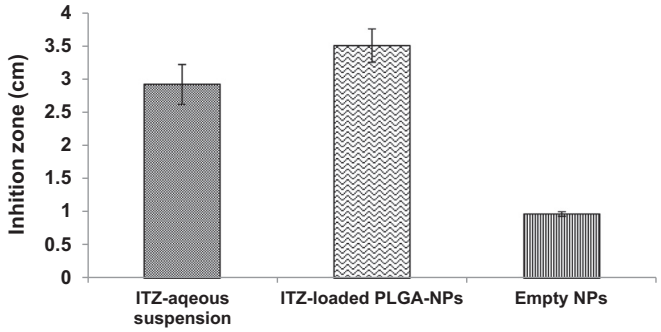

Fig. 6. Antifungal activity comparison of different ITZ containing formulations against *Candida albicans*, results were represented as mean ± SD, $n = 3$.

temperature. The results of stability studies revealed that ITZ-loaded PLGA-NPs were found to be stable at 30 ± 1 °C for a period of 3 months. No major changes were found in the selected physical characterization parameters for the stored PLGA-NPs (Table 2). The particle size of NPs were slightly increased but the changes were not significant, which might be due to the environmental protection effect of TPGS as stabilizer on covering of the NPs (Kalam et al., 2017; Li et al., 2017).

5. Conclusion

PLGA-NPs stabilized by TPGS and encapsulated with ITZ were successfully utilized to render stable nano-size drug loaded particles. Nanoprecipitation method, however, was superior over the other methods in terms of morphology, particle size, zeta potential, encapsulation efficiency and drug loading capacity. ITZ nanosuspension release profile was better as compared to lyophilized or spray-dried NPs. Antifungal activity of ITZ loaded NPs was slightly improved compared to the ITZ-aqueous suspension. TPGS proved to be an effective stabilizer as well as permeation enhancer, which could result in higher encapsulation and drug loading NPs. Briefly, the PLGA-NPs stabilized by TPGS system considerably would improve the bioavailability of ITZ by enhanced aqueous dispersibility of the drug and intestinal permeability, which in turn would improve its antifungal activity. Thus, above nano-system would be an outstanding choice for the treatment of fungal infections because of high efficacy.

Conflict of interest

"None".

Acknowledgment

"The authors extend their appreciation to the Deanship of Scientific Research at King Saud University for funding this work through research group no (RG-1436-027)".

References

Akhtar, M.J., Ahamed, M., Alhadlaq, H.A., Alshamsan, A., 2017. Nanotoxicity of cobalt induced by oxidant generation and glutathione depletion in MCF-7 cells. Toxicol. in Vitro 40, 94–101.

Alomrani, A.H., Shazly, G.A., Amara, A.A., Badran, M.M., 2014. Itraconazole-hydroxypropyl-beta-cyclodextrin loaded deformable liposomes: *in vitro* skin penetration studies and antifungal efficacy using *Candida albicans* as model. Colloids Surf. B: Biointerfaces 121, 74–81.

Alshamsan, A., 2014. Nanoprecipitation is more efficient than emulsion solvent evaporation method to encapsulate cucurbitacin I in PLGA nanoparticles. Saudi Pharm J. 22, 219–222.

Altamimi, M.A., Neau, S.H., 2016. Use of the Flory-Huggins theory to predict the solubility of nifedipine and sulfamethoxazole in the triblock, graft copolymer Soluplus. Drug Dev. Ind. Pharm. 42, 446–455.
Altamimi, M.A., Neau, S.H., 2017. Investigation of the *in vitro* performance difference of drug-Soluplus(R) and drug-PEG 6000 dispersions when prepared using spray drying or lyophilization. Saudi Pharm J. 25, 419–439.
Bernabeu, E., Helguera, G., Legaspi, M.J., Gonzalez, L., Hocht, C., Taira, C., Chiappetta, D.A., 2014. Paclitaxel-loaded PCL-TPGS nanoparticles: *in vitro* and *in vivo* performance compared with Abraxane(R). Colloids Surf. B: Biointerfaces 113, 43–50.
Binkhathlan, Z., Lavasanifar, A., 2013. P-glycoprotein inhibition as a therapeutic approach for overcoming multidrug resistance in cancer: current status and future perspectives. Curr. Cancer Drug Targets 13, 326–346.
Bootman, J.L., 1998. Cost-effectiveness of two new treatments for onychomycosis: an analysis of two comparative clinical trials. J. Am. Acad. Dermatol. 38, S69–S72.
Brannon-Peppas, L., Blanchette, J.O., 2004. Nanoparticle and targeted systems for cancer therapy. Adv. Drug Deliv. Rev. 56, 1649–1659.
Desai, M.P., Labhasetwar, V., Amidon, G.L., Levy, R.J., 1996. Gastrointestinal uptake of biodegradable microparticles: effect of particle size. Pharm. Res. 13, 1838–1845.
Dutkiewicz, Hage, 2010. Aspergillus infections in the critically ill. Proc Am Thorac Soc. 7 (3), 204–209. https://doi.org/10.1513/pats.200906-050AL.
Fonseca, C., Simoes, S., Gaspar, R., 2002. Paclitaxel-loaded PLGA nanoparticles: preparation, physicochemical characterization and *in vitro* anti-tumoral activity. J. Control. Release 83, 273–286.
Gajra, B., Dalwadi, C., Patel, R., 2015. Formulation and optimization of itraconazole polymeric lipid hybrid nanoparticles (Lipomer) using Box Behnken design. Daru 23, 3.
Gaonkar, R.H., Ganguly, S., Dewanjee, S., Sinha, S., Gupta, A., Chattopadhyay, D., Chatterjee Debnath, M., 2017. Garcinol loaded vitamin E TPGS emulsified PLGA nanoparticles: preparation, physicochemical characterization, *in vitro* and *in vivo* studies. Sci. Rep. 7, 530.
Hans, M.L., Lowman, A.M., 2002. Biodegradable nanoparticles for drug delivery and targeting. Curr. Opinion Solid State Mater. Sci. 6, 319–327.
Hawksworth, 2001. The magnitude of fungal diversity: the 1.5 million species estimate revisited. Mycol. Res. 105 (12), 1422–1432.
Heykants, J., Van Peer, A., Van de Velde, V., Van Rooy, P., Meuldermans, W., Lavrijsen, K., Woestenborghs, R., Van Cutsem, J., Cauwenbergh, G., 1989. The clinical pharmacokinetics of itraconazole: an overview. Mycoses 32 (Suppl. 1), 67–87.
Huang, J., Wigent, R.J., Schwartz, J.B., 2008. Drug-polymer interaction and its significance on the physical stability of nifedipine amorphous dispersion in microparticles of an ammonio methacrylate copolymer and ethylcellulose binary blend. J. Pharm. Sci. 97, 251–262.
Islam, T.A., Majid, F., Ahmed, M., Afrin, S., Jhumky, T., Ferdouse, F., 2018. Prevalence of dermatophytic infection and detection of dermatophytes by microscopic and culture methods. J. Enam Med. Coll. 8, 11–15.
Jung, J.Y., Yoo, S.D., Lee, S.H., Kim, K.H., Yoon, D.S., Lee, K.H., 1999. Enhanced solubility and dissolution rate of itraconazole by a solid dispersion technique. Int. J. Pharm. 187, 209–218.
Kalam, M.A., Alshamsan, A., 2017. Poly (d, L-lactide-*co*-glycolide) nanoparticles for sustained release of tacrolimus in rabbit eyes. Biomed. Pharmacother. 94, 402–411.
Kalam, M.A., Alshehri, S., Alshamsan, A., Haque, A., Shakeel, F., 2017. Solid liquid equilibrium of an antifungal drug itraconazole in different neat solvents: Determination and correlation. J. Mol. Liq. 234, 81–87.
Leroux, J.-C., Allemann, E., De Jaeghere, F., Doelker, E., Gurny, R., 1996. Biodegradable nanoparticles-from sustained release formulations to improved site specific drug delivery. J. Control. Release 39, 339–350.
Li, Z., Tao, W., Zhang, D., Wu, C., Song, B., Wang, S., Wang, T., Hu, M., Liu, X., Wang, Y., Sun, Y., Sun, J., 2017. The studies of PLGA nanoparticles loading atorvastatin calcium for oral administration *in vitro* and *in vivo*. Asian J. Pharmaceut. Sci. 12, 285–291.
Ling, X., Huang, Z., Wang, J., Xie, J., Feng, M., Chen, Y., Abbas, F., Tu, J., Wu, J., Sun, C., 2016. Development of an itraconazole encapsulated polymeric nanoparticle platform for effective antifungal therapy. J. Mater. Chem. B 4, 1787–1796.
Mainardes, R.M., Evangelista, R.C., 2005. Praziquantel-loaded PLGA nanoparticles: preparation and characterization. J. Microencapsul. 22, 13–24.
McCall, R.L., Sirianni, R.W., 2013. PLGA nanoparticles formed by single- or double-emulsion with vitamin *E*-TPGS. J. Vis. Exp. 51015.
McCarron, P.A., Donnelly, R.F., Marouf, W., 2006. Celecoxib-loaded poly(D,L-lactide-*co*-glycolide) nanoparticles prepared using a novel and controllable combination of diffusion and emulsification steps as part of the salting-out procedure. J. Microencapsul. 23, 480–498.
Mittal, G., Sahana, D.K., Bhardwaj, V., Ravi Kumar, M.N., 2007. Estradiol loaded PLGA nanoparticles for oral administration: effect of polymer molecular weight and copolymer composition on release behavior *in vitro* and *in vivo*. J. Control. Release 119, 77–85.
Modi, A., Tayade, P., 2006. Enhancement of dissolution profile by solid dispersion (kneading) technique. AAPS PharmSciTech 7, 68.
Mohamed, F., van der Walle, C.F., 2008. Engineering biodegradable polyester particles with specific drug targeting and drug release properties. J. Pharm. Sci. 97, 71–87.
Nagarwal, R.C., Kant, S., Singh, P.N., Maiti, P., Pandit, J.K., 2009. Polymeric nanoparticulate system: a potential approach for ocular drug delivery. J. Control. Release 136, 2–13.
Nakarani, M., Misra, A.K., Patel, J.K., Vaghani, S.S., 2010. Itraconazole nanosuspension for oral delivery: Formulation, characterization and *in vitro* comparison with marketed formulation. Daru 18, 84–90.
Nesseem, D.I., 2001. Formulation and evaluation of itraconazole *via* liquid crystal for topical delivery system. J. Pharm. Biomed. Anal. 26, 387–399.
Papadimitriou, S., Bikiaris, D., 2009. Novel self-assembled core-shell nanoparticles based on crystalline amorphous moieties of aliphatic copolyesters for efficient controlled drug release. J. Control. Release 138, 177–184.
Patel, N.R., 2010. Itraconazole Loaded Poly (lactic-*co*-glycolic) Acid Nanoparticles for Improved Antifungal Activity. Louisiana State University.
Patel, N.R., Damann, K., Leonardi, C., Sabliov, C.M., 2010. Itraconazole-loaded poly (lactic-*co*-glycolic) acid nanoparticles for improved antifungal activity. Nanomedicine (London) 5, 1037–1050.
Pinner, R.W., Teutsch, S.M., Simonsen, L., Klug, L.A., Graber, J.M., Clarke, M.J., Berkelman, R.L., 1996. Trends in infectious diseases mortality in the United States. JAMA 275, 189–193.
Qiu, L., Hu, B., Chen, H., Li, S., Hu, Y., Zheng, Y., Wu, X., 2015. Antifungal efficacy of itraconazole-loaded TPGS-b-(PCL-ran-PGA) nanoparticles. Int. J. Nanomedicine 10, 1415–1423.
Rabinow, B.E., 2004. Nanosuspensions in drug delivery. Nat. Rev. Drug Discov. 3, 785–796.
Richardson, 2005. Changing patterns and trends in systemic fungal infections. J Antimicrob Chemother 56 (Suppl 1), i5–i11.
Sahana, D.K., Mittal, G., Bhardwaj, V., Kumar, M.N., 2008. PLGA nanoparticles for oral delivery of hydrophobic drugs: influence of organic solvent on nanoparticle formation and release behavior *in vitro* and *in vivo* using estradiol as a model drug. J. Pharm. Sci. 97, 1530–1542.
Sathigari, S.K., Radhakrishnan, V.K., Davis, V.A., Parsons, D.L., Babu, R.J., 2012. Amorphous-state characterization of efavirenz–polymer hot-melt extrusion systems for dissolution enhancement. J. Pharm. Sci. 101, 3456–3464.
Shieh, M.J., Hsu, C.Y., Huang, L.Y., Chen, H.Y., Huang, F.H., Lai, P.S., 2011. Reversal of doxorubicin-resistance by multifunctional nanoparticles in MCF-7/ADR cells. J. Control. Release 152, 418–425.
Soppimath, K.S., Aminabhavi, T.M., Kulkarni, A.R., Rudzinski, W.E., 2001. Biodegradable polymeric nanoparticles as drug delivery devices. J. Control. Release 70, 1–20.
Tao, T., Zhao, Y., Wu, J., Zhou, B., 2009. Preparation and evaluation of itraconazole dihydrochloride for the solubility and dissolution rate enhancement. Int. J. Pharm. 367, 109–114.
Wang, Y., Liu, X., Liu, G., Guo, H., Li, C., Zhang, Y., Zhang, F., Zhao, Z., Cheng, H., 2016. Novel galactosylated biodegradable nanoparticles for hepatocyte-delivery of oridonin. Int. J. Pharm. 502, 47–60.
Zheng, W.S., Fang, X.Q., Wang, L.L., Zhang, Y.J., 2012. Preparation and quality assessment of itraconazole transfersomes. Int. J. Pharm. 436, 291–298.
Zolnik, B.S., Burgess, D.J., 2007. Effect of acidic pH on PLGA microsphere degradation and release. J. Control. Release 122, 338–344.
Zong, L., Li, X., Wang, H., Cao, Y., Yin, L., Li, M., Wei, Z., Chen, D., Pu, X., Han, J., 2017. Formulation and characterization of biocompatible and stable I.*V.* itraconazole nanosuspensions stabilized by a new stabilizer polyethylene glycol-poly(beta-Benzyl-L-aspartate) (PEG-PBLA). Int. J. Pharm. 531, 108–117.